Lab on a Chip

Cite this: *Lab Chip*, 2012, **12**, 1629

www.rsc.org/loc

PAPER

Rapid screening of antibiotic toxicity in an automated microdroplet system†

Krzysztof Churski,[a] Tomasz S. Kaminski,[a] Slawomir Jakiela,[a] Wojciech Kamysz,[b] Wioletta Baranska-Rybak,[c] Douglas B. Weibel[d] and Piotr Garstecki*[a]

Received 22nd December 2011, Accepted 7th February 2012
DOI: 10.1039/c2lc21284f

We report an automated microfluidic platform for 'digitally' screening the composition space of droplets containing cocktails of small molecules and demonstrate the features of this system by studying epistatic interactions between antibiotics and *Escherichia coli* ATCC 25922. This system has several key characteristics: (i) it uses small (<100 μL) samples of liquids and suspensions of bacteria that are introduced directly into the chip; (ii) it generates a sequence of droplets with compositions, including reagents and bacterial cell suspensions that are programmed by the user; (iii) it exports the sequence of droplets to an external segment of tubing that is subsequently disconnected for incubation and storage; and (iv) after incubation of bacteria in droplets, the droplets are injected into a second device equipped with an in-line fiber optic spectrophotometer that measures cell growth. The system generates and fuses droplets with precise (<1% in standard deviation) control of liquid volumes and of the concentrations of input substrates. We demonstrate the application of this technology in determining the minimum inhibitory concentration and pair-wise interactions of ampicillin, tetracycline, and chloramphenicol against *E. coli*. The experiments consumed small volumes of reagents and required minutes to create the droplets and several hours for their incubation and analysis.

Introduction

We demonstrate an automated microfluidic system that generates sequences of droplets each of which has a volume of ~1 μL and consists of a unique preprogrammed composition of reagents and cells (*e.g.* bacteria, nutrients, growth indicator, and antibiotics). Small volumes of liquid samples (single to tens of μL) are introduced into the device using a pipette and are subsequently split into microdroplets (volume, 100 nL–2 μL) according to a pre-programmed fluid handling protocol. The microfluidic system controls the composition of the droplets over time by splitting and merging them together. The resulting device provides new opportunities for rapidly screening conditions for chemical and microbiological experiments.

To demonstrate the salient advantages of this technique for bacterial studies, we used the system to create microdroplets containing bacteria and different concentrations of the antibiotics: ampicillin, chloramphenicol and tetracycline. After encapsulating cells admixed with nutrient media and antibiotics, we transferred spatially encoded sequences of microdroplets to external tubing for storage, disconnected the tubing, and incubated it at 37 °C to promote cell growth. Following incubation, we used pressure-driven flow to transfer microdroplets into a device containing an on-chip spectrophotometer where we measured the viability of bacterial cells, the minimum inhibitory concentrations (MIC) of the antibiotics, and epistatic interactions between the small molecules. Experiments consisting of hundreds of parallel microdroplets with varying chemical compositions required less than 10 min to prepare and provide a rapid alternative for microbiological assays and screens that are relevant to clinical laboratories.

Limitations of microbiological assays

The excessive application of antibiotics in medicine, veterinary science, and the food industry has played a central role in the growing threat of bacterial drug resistance.[1,2] Counter-measures for treating drug resistance *via* the introduction of new antimicrobial compounds have been slow to emerge. Considerable interest has been placed in developing cocktails of existing antibiotics that may transcend the complications associated with introducing new antibiotics to the market.[3] A challenge in this area hinges upon the complexity of screening a very broad chemical space for mixtures of antibiotics at a wide range of concentrations to identify synergistic doses that are lethal and yet

[a]*Institute of Physical Chemistry, Polish Academy of Sciences, Kasprzaka 44/52, 01-224 Warsaw, Poland. E-mail: garst@ichf.edu.pl*
[b]*Department of Inorganic Chemistry, Faculty of Pharmacy, Medical University of Gdansk, Hallera 107, 80-416 Gdansk, Poland*
[c]*Department of Dermatology, Venerology and Allergology, Faculty of Medicine, Medical University of Gdansk, Debinki 7, 80-211 Gdansk, Poland*
[d]*Department of Biochemistry, University of Wisconsin-Madison, 433 Babcock Drive, Madison, WI 53706, USA*
† Electronic supplementary information (ESI) available: Results of the test for cross-contamination between microdroplets. See DOI: 10.1039/c2lc21284f

minimize drug resistance. Classical techniques that center upon pipetting and other manual methods of fluid handling have validated this approach for multidrug treatment and have provided insight into other areas of microbiology, including ecology and evolution.[4–6] Conventional mechanisms of fluid handling limit the cost and throughput of these experiments and the chemical space that can be explored.

The introduction of methods for improving the throughput of fluid handling may facilitate the exploration of chemical space and the identification of potent antibiotic cocktails. Here, we demonstrate a microfluidic system that improves the throughput of toxicity assays of antibiotic cocktails against the model bacterium *Escherichia coli*. The device consumes small amounts of reagents and enables hundreds of experiments to be performed simultaneously. In addition to facilitating chemical and microbiological studies, the device enables multidrug profiling of microbial pathogens and the rapid determination of effective treatments for bacterial sepsis in clinical settings.

Incubation of bacteria in microfluidics

Microfluidic techniques improve the rate of growth and the detection of bacterial strains compared to traditional microbiological techniques.[7–11] Droplet microfluidic systems have several unique characteristics that provide an advantage for microbiological applications, including: (i) minimizing the contamination between samples; (ii) rapid mixing within droplets; (iii) reproducibly forming droplets that have a precise volume; and (iv) containing reactions in small volumes of liquid.[12,13] We have recently demonstrated an automated technique for creating microdroplets in a microfluidic device that uses external valves and thereby minimizes the complexity and cost of the system, as it is compatible with devices fabricated in virtually any material.[14] In this technique, active control of the flow of both the discontinuous and the continuous liquids enables us to form microdroplets with a wide range of volumes.[14]

Passing the liquid samples through large, external electromagnetic valves has several drawbacks, including (i) limiting the minimum sample volume to several mL; (ii) challenges in preparing multiple samples in a sequence without cross-contamination; and (iii) the potential for overheating samples and their contact with components of the valve. To transcend these limitations, we introduce a technique that requires one fluid-handling step, in which the user introduces small sample volumes (*e.g.* >1 μL) directly on the chip using a pipette. Using hexadecane as the continuous phase, pressure driven flow introduces the samples into the network of channels where they are split, fused, and mixed. The integration of multiple, parallel microdroplet generators in one device makes it possible for us to use small samples of liquids to perform multidimensional screens in which we alter the concentration of three antibiotics and measure their effects on *E. coli* cell growth.

Results

Design and operation of the system

The device consisted of four microfluidic T-junctions for creating microdroplets simultaneously and in parallel (Fig. 1). The channels at the junction were 400 μm wide and 400 μm tall. We deposited fluid samples into reservoir channels that were 1 mm wide and 1 mm tall and accommodated a port for a pipette tip. The reservoir channels tapered to 400 μm wide and 400 μm tall at a distance approximately 1 cm upstream of the T-junctions. Each sample inlet port consisted of a vertical hole that was 1 mm in diameter and terminated in a circular groove that housed an O-ring seal (I.D. 0.78 mm, O.D. 2.78 mm). We sealed the ports using an external screw to seat a flat piece of polycarbonate against the O-ring. We connected the upstream inlets of the two channels leading to the T-junction to external valves using resistive steel capillaries (O.D. 400 μm, I.D. 205 μm, Mifam, Poland).

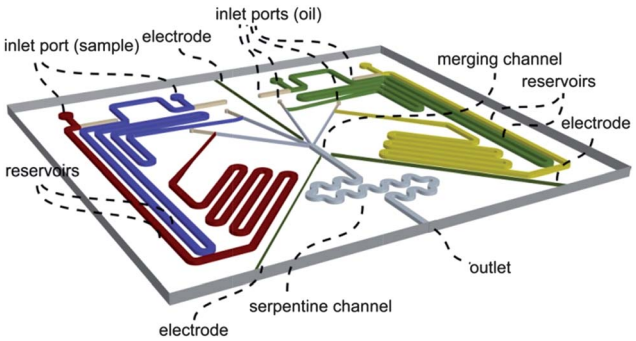

Fig. 1 A schematic diagram of the microfluidic device used in the experiments. *Legend*: (i) red, blue, green, and yellow channels depict sample reservoirs; (ii) light brown channels depict channels filled with hexadecane; (iii) grey channels are downstream channels; and (iv) dark green lines depict electrodes.

We actuated fluid flow using solenoid valves (V165, Sirai, Italy). The valves controlling the flow of the continuous phase (hexadecane containing 2% Span 80) were connected to a pressurized reservoir of hexadecane maintained at 600 mbar. Similarly, the valves controlling the flow of samples were connected to a second pressurized reservoir (280 mbar). The reservoirs were connected to the valves *via* polyurethane tubing (O.D. 4 mm, I.D. 2 mm). Each reservoir was supplied with compressed air *via* precision pressure regulators (series PR1-RGP, G 1/4, Bosch Rexroth AG, Germany) that were connected in series.

The outlets of the four T-junctions were connected to a channel (1.2 mm wide, 1.0 mm tall) that led to a wide channel (800 μm wide, 800 μm tall). The chamber was equipped with three electrodes (see Fig. 1) connected to an AC source (2 kV, 100 Hz, Trek Model 609E-6, USA). The oscillation of the electric field regulated the rate of coalescence of droplets emerging from individual T-junctions.[15–18]

Merged droplets flowed through a serpentine-shaped outlet that facilitated mixing and through the outlet port of the device. The outlet port was connected to a short (10 cm) section of PE60 polyethylene tubing (O.D. 1.22 mm, I.D. 0.76 mm, Becton Dickinson, USA) that was connected to a 2 cm long segment of PE160 (O.D. 1.58 mm, I.D. 1.2 mm). This makeshift connector enabled us remove and replace long (0.5–2 m) sections of PE60 tubing that we used for the storage and incubation of sequences of microdroplets—this operation was easy and error-free providing for robust and rapid exchange of the tubings. We found it practical to fill each tubing with a sequence of up to 70 droplets. Longer sequences introduced resistance to flow that

began to slightly influence the process and precision of formation of droplets.

Aspiration of samples

Fig. 2 depicts an individual T-junction and illustrates the port for the pipette tip. We started experiments with the inlet ports closed. We filled the entire device with hexadecane by opening all the valves and then closing them. Once the chip was filled with hexadecane we loosened one of the clamps and removed the polycarbonate slab and the rubber O-ring. With the port open, we inserted a pipette tip into the inlet port and released a small bolus of air that pushed out the hexadecane in the port and prevented the cross-contamination of our sample with material from previous experiments. We then loaded our sample using the pipette and closed the port by seating the O-ring using the polycarbonate slab and the clamp. We filled all the reservoirs with the other liquid samples in the same way.

Generation of droplets from samples of different viscosities

Microfluidic systems that use a constant inflow of immiscible liquids into junctions (*e.g.* flow-focusing[19–22] or T-junction[23–28]) can produce monodisperse droplets. At low values of the capillary number, the volume of the droplets depends[21,22,24,25,27,28] on the material parameters of the liquids, such as interfacial tension between the immiscible phases and their viscosities. The volume of the droplets and the threshold rate of flow for the transition between dripping and jetting also depend on these parameters.[29] These characteristics complicate the production of droplets of required volume from samples of diverse viscosities in microfluidic droplet generators. This limitation is particularly germane to the production of individual predefined volumes of liquid from arbitrary samples in automated systems.

We have demonstrated recently[30] that active control of the flow of the two immiscible phases expands the range of flow rates in which the system produces droplets without transitioning to the jetting regime. The system that we describe here is equipped with on-chip reservoirs for samples and alleviates the dependence of viscosity on droplet volume: the samples are small and contained in reservoir channels of relatively large cross-section and small resistance and are actuated by the flow of hexadecane. The rate of flow of hexadecane is controlled[31] by the pressure head between the pressurized reservoir and the resistance $R_{capillary}$ of the resistive capillary positioned between the valve and the chip, and the hydraulic resistance R_{chip} of the chip. We tune $R_{capillary}$ to be much larger than R_{chip}. For hexadecane as the continuous liquid (viscosity $\mu_{oil} = 3.0 \pm 0.1$ mPa s) and a capillary of internal diameter $D = 205$ μm and length $L = 5$ m (or $L = 10$ m), $R_{capillary} = 3.45 \times 10^{14}$ (6.9×10^{14}) Pa s m^{-3}. We can estimate $R_{chip} \approx 8\mu_{sample}L_{reservoir}\pi^{-1}r_{reservoir}^{-4} + 8\mu_{oil}L_{oil}\pi^{-1}r_{oil}^{-4}$, assuming that the resistance of the outlet channel is approximately proportional to the viscosity of the continuous liquid. This estimate yields $R_{chip} = 4.0 \times 10^{11}$ Pa s m^{-3} for $\mu_{sample} = 1$ mPa s, $R_{chip} = 7.15 \times 10^{11}$ Pa s m^{-3} for $\mu_{sample} = 3$ mPa s and $R_{chip} = 1.60 \times 10^{13}$ Pa s m^{-3} for $\mu_{sample} = 100$ mPa s. As these values are significantly smaller than $R_{capillary}$, the rate of flow of oil through the capillary—and hence the speed of the plug of liquid sample in the reservoir—depends weakly on μ_{sample}.

Fig. 2 shows the volumes of microdroplets generated in our system from liquid samples with viscosities ranging from 1 mPa s to 100 mPa s. Low viscosity liquids (1–3 mPa s in the example) have no influence on droplet volume, which makes this technique particularly attractive for biochemical and microbiological experiments in which most samples can be manipulated without having to calibrate the device for each sample. Higher viscosity liquids shift the volume of microdroplets (see data for 30 and 100 mPa s in Fig. 2). This relationship may arise from a mobility[32] that is significantly smaller than unity for droplets that have a larger viscosity than the continuous liquid. Viscous samples can be transformed into droplets and the relation between microdroplet volume and the interval τ_{open} is linear. This relationship enables the rapid calibration of the system *via* determining the volumes for at least two different values of τ_{open}.

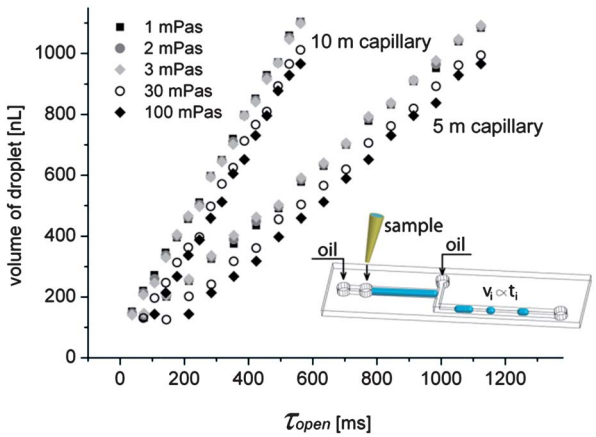

Fig. 2 The dependence of the volume of droplet on τ_{open} of the valve for (i) five fluids of five different viscosities (1, 2, 3, 30 and 100 mPa s); and (ii) two lengths of resistive capillary (5 and 10 m). The pressure of oil was 500 mbar, the pressure of water was 300 mbar (for 5 m capillary), and the pressure of water was 600 mbar (for 10 m capillary). The cartoon inset depicts the system for sample aspiration.

Generation of sequences of mixtures

The microfluidic system is illustrated in Fig. 3. After loading samples onto the chip, the automated protocol sequentially pushes the samples to the T-junctions. After a small volume of the sample passes into the junction, the device stops the flow of the sample and opens the flow of hexadecane for several seconds. The small volume of fluid in the T-junction breaks off and is flushed from the system while the front of the sample plug remains positioned at the entrance of the T-junction, ready to generate droplets on demand.

After priming the system, we create droplets on demand of predetermined volumes using the protocol reported previously.[14] In summary, we stop the flow of hexadecane at each junction simultaneously, open the flow of the sample (pushed with hexadecane) for a time interval τ_{ij}, where i corresponds to the index of the sample and j to the number of the droplet, and push a sample volume v_{ij} into the main channel of the T-junction. After the requisite sample volumes are pushed into the junctions, the flow of hexadecane begins, microdroplet break-off occurs, and the microdroplets are moved forward and their entry into the

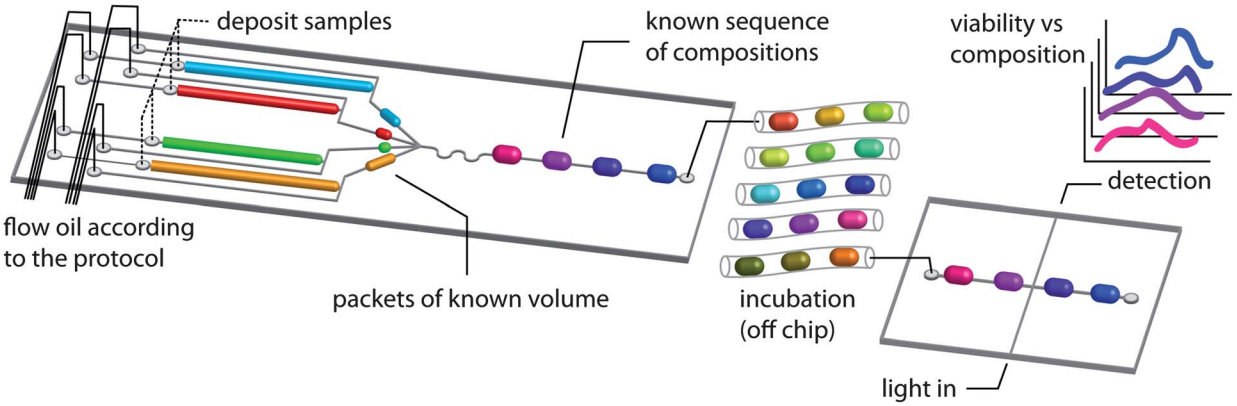

Fig. 3 A schematic diagram depicting the operation of the microfluidic system. We generated packets of microdroplets of known volume and merged them to create microdroplets with a defined composition. The sequence of microdroplets formed in the device was stored in polyethylene tubing and incubated off-chip. After incubation, the microdroplets were loaded into a microchannel connected to an excitation lamp and a spectrophotometer *via* optical fibers where we detected the intensity (and hence concentration) of a reagent present that indicated the metabolism of bacteria.

merging chamber is synchronized. The AC electric field across the chamber is simultaneously applied to facilitate the merging of droplets *via* electrocoalescence.[15–18]

To test the precision of the system for preparing mixtures of predefined composition, we loaded distilled water, an aqueous solution of methylene blue (10^{-5} M), and an aqueous solution of tartrazine (10^{-5} M) into the reservoirs of three T-junctions. We operated the device using a protocol that generated a sequence of 121 microdroplets that screened an 11 × 11 matrix of concentrations of the two dyes. We measured the absorbance of methylene blue ($\lambda = 665$ nm) and tartrazine ($\lambda = 425$ nm) and used Beer's law to determine the concentration of the dyes in drops containing mixtures of the two compounds. The maximum relative error between the measured values and preprogrammed concentrations was less than 1%. It was calculated according to the following equation: $S_{\text{error}}(\%) = 100\max\left(|c_i^{\text{meas}} - c_i^{\text{fixed}}|/c_i^{\text{fixed}}\right)$, where S_{error} is the maximum relative error of concentration, c_i^{meas} the i-th measured concentration of the dye, and c_i^{fixed} the i-th fixed concentration of the dye. Fig. 4 shows the concentrations measured in three repeated experiments and a grid depicting the different combinations.

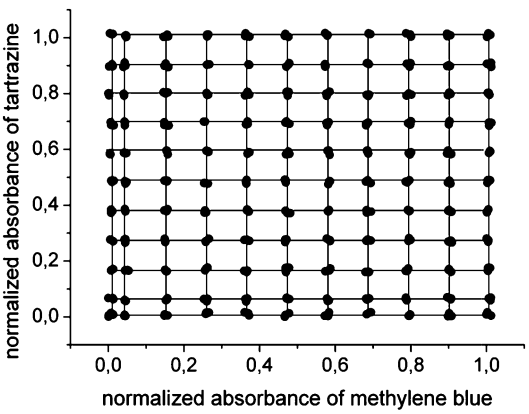

Fig. 4 A plot of the normalized absorbance of methylene blue and tartrazine measured from 3 identical sequences of 121 droplets. The absorbances of methylene blue and tartrazine were measured at $\lambda = 665$ nm and 425 nm, respectively.

Testing toxicity of cocktails of antibiotics

We used the system depicted in Fig. 3 to encapsulate cells of *E. coli* strain ATCC 25922 admixed with growth media, antibiotics, and resazurin; this compound is metabolized by bacteria to produce the fluorescent compound resorufin, and is thus a convenient indicator of metabolism. In each experiment we loaded the on-chip reservoirs with the liquid samples, closed the ports, and initiated an automated protocol that first pushed the samples towards T-junctions and then generated a sequence of microdroplets with preprogrammed compositions. We collected the sequence of microdroplets in a section of tubing. After the system had generated the sequence, we disconnected the tubing and stored it in an incubator (Binder BD 23, Germany) at 37 °C. We loaded the system with new samples and added a new section of tubing to the device, which was then used to generate a new sequence of microdroplets.

Following 3 h of incubation we connected one end of the tubing to a syringe pump (Harvard Apparatus PHD 2000, USA) and the other end to an inlet of a microfluidic device that housed an on-chip fiber optic spectrophotometer (Fig. 3). We illuminated the droplets with green laser ($\lambda = 532$ nm, 50 mW) through an optical path of 0.76 mm and measured the fluorescence spectra with a spectrophotometer (Ocean Optics, USB 2000+). The flow rate at which we typically pushed the droplets through the optic cell was ~10 mL h^{-1}, resulting in a dwell time of ~0.8 s for each microdroplet in the laser line. The system collected the absorbance spectra at a frequency of 100 Hz and enabled us to measure ~80 spectra for each microdroplet, while providing a reliable analysis of the fluorescence intensity of resorufin. We averaged the value of fluorescence at $\lambda = 580$ nm using 50 spectra per microdroplet recorded from the middle of the droplet. We disregarded the spectra from the front and from the end of the droplets as the curvature of these regions can distort the spectra.

Preventing the cross-contamination of antibiotics between droplets

We verified that no cross-contamination occurred between microdroplets in a sequence, *i.e.* neither resazurin (or resorufin)

nor the antibiotic diffused between microdroplets. We prepared a sequence of seven microdroplets of which the first three contained resazurin (44 μM) and bacteria (~5 × 10^5 CFU mL^{-1}), one microdroplet contained a high concentration of chloramphenicol and tetracycline (2 mg L^{-1} and 0.5 mg L^{-1} respectively) and no cells; and three microdroplets contained only bacteria (~5 × 10^5 CFU mL^{-1}). We incubated the sequence of microdroplets for 3 h at 37 °C and measured the fluorescence intensity of resorufin (λ = 580 nm). We observed no significant difference between the fluorescence intensities of the first three droplets and no fluorescence in the other four (Fig. S1, ESI†).

Determination of the minimum inhibitory concentration of antibiotics against *E. coli*

Using the microfluidic system we determined the MIC of ampicillin (inhibits cell wall synthesis), chloramphenicol and tetracycline (both inhibit protein translation) against *E. coli* ATCC 25922. In each MIC experiment, we deposited a suspension of *E. coli* (7 × 10^6 CFU mL^{-1}) into the channel labeled 'B' in Fig. 5. We deposited solutions of antibiotics in channels $C^{A/10}$ and C^{A} (2.8 and 28 mg L^{-1} for ampicillin, 0.7 and 7 mg L^{-1} for chloramphenicol, and 0.28 and 2.8 mg L^{-1} for tetracycline). We introduced liquid growth media in the channel labeled 'M'. The solutions of antibiotic and liquid growth media contained resazurin (44 μM).

Once the chip was loaded and prepared for use, we generated synchronized packets of microdroplets containing: (i) a fixed volume (100 nL) of a suspension of bacteria; (ii) varying volumes of $C^{A/10}$ and C^{A} (between 0 and 1.3 μL); and (iii) a varying volume of the nutrient media to achieve a constant volume of 1.4 μL for the incubation mixture. Our MIC screen consisted of generating a sequence of 49 droplets containing a geometric progression of antibiotic concentration (in 1.1× increments of concentration). The first microdroplet in the series consisted of bacteria (100 nL) and 1.3 μL of nutrient media. To achieve a concentration range across the subsequent microdroplets, the volume of droplets in channel $C^{A/10}$ was increased from 0 to 1.3 μL (with M decreasing from 1.3 μL to 0). We then closed channel $C^{A/10}$ and increased the volume of the C^{A} droplets from 0 to 1.3 μL while droplets containing nutrient media were decreased in volume from 1.3 μL to 0. The final concentrations of antibiotics in the microdroplets varied between 0.2 and 20 mg L^{-1} (ampicillin), 0.05–5.0 mg L^{-1} (chloramphenicol), and 0.02–2.0 mg L^{-1} (tetracycline).

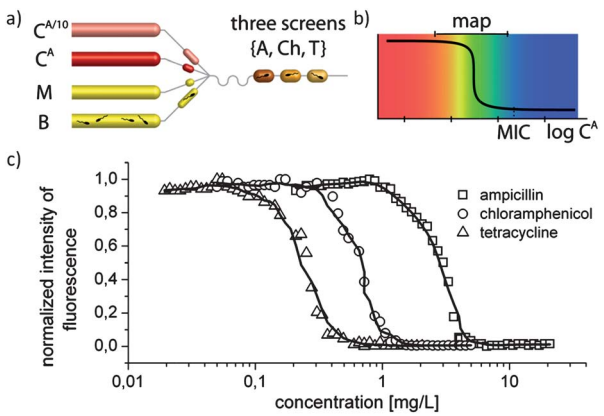

Fig. 5 A schematic diagram depicting the configuration of samples in the reservoirs (a), the expected dependence of fluorescence intensity of resorufin on antibiotic concentration (b), and the measured dependence of the normalized intensity of resorufin fluorescence on the concentration of ampicillin, chloramphenicol, and tetracycline (c). The color-coding shown in the scheme (b) is later used in the maps of interactions between pairs of antibiotics.

It took approximately 5 min to load the system with solutions and prepare it for generating the sequence of microdroplets. Microdroplet formation required operating the device for approximately 100 s. After 3 h of incubation, we measured the intensity of fluorescence from resorufin in each droplet and normalized these values to the intensity of the droplet with the highest intensity of fluorescence. Fig. 5 illustrates the normalized intensity as a function of the antibiotic concentration. From these data we determined the following MIC values: 5.0 mg L^{-1} for ampicillin, 1.8 mg L^{-1} for chloramphenicol, and 0.6 mg L^{-1} for tetracycline hydrochloride.

As a control for our measurements we tested the susceptibility of *E. coli* ATCC 25922 to a concentration range of ampicillin, chloramphenicol, and tetracycline (varied from 0.006 to 32 mg L^{-1}) using the classic 2-fold serial dilution technique in tubes. We performed each MIC measurement in duplicate and determined the following MIC values: 4 mg L^{-1} for ampicillin, 4 mg L^{-1} for chloramphenicol, and 0.5 mg L^{-1} for tetracycline hydrochloride. These values are in excellent agreement with the values determined using the microdroplet protocol and with values reported in the literature (4.0 mg L^{-1} (ref. 33), 4.0 mg L^{-1} (ref. 33), 0.5 mg L^{-1} (ref. 34) respectively).

Determination of pairwise epistatic interactions between antibiotics

We used the MIC values determined for the three antibiotics to select a concentration range for each antibiotic that would be relevant for mapping the profile of its interactions. Specifically, we varied the concentration of ampicillin from 0 to 5 mg L^{-1} in 0.5 mg L^{-1} increments; chloramphenicol from 0 to 2 mg L^{-1} in 0.2 mg L^{-1} increments; and tetracycline from 0 to 0.5 mg L^{-1} in 0.05 mg L^{-1} increments. In these experiments we used the channel labeled 'B' (Fig. 5) to create microdroplets using microdroplets of bacteria of fixed volume (100 nL), channels labeled C^{A1} and C^{A2} to generate microdroplets (100 nL–1 μL) consisting of solutions of two different antibiotics, and the channel labeled 'M' to generate microdrops of liquid culture media. These droplets were fused to create microdroplets with a volume of 2.1 μL for incubation. We programmed the device to create 121 different combinations of two antibiotics at different concentrations that evenly covered an 11 × 11 matrix of compositions. The device created the microdroplets at a frequency of 0.5 Hz. The total time for making of the sequence of microdroplets and transferring them into polyethylene tubing for incubation was 4 min. After incubation for 3 h, we transferred the droplets to an on-chip spectrophotometer and measured their fluorescence.

Fig. 6 shows the results of these experiments. We identified three different types of interactions that are based on the definition of Loewe additivity.[3,35,36] Loewe additivity states that if the activities of two antibiotics are additive, the combined level of

inhibition is the sum of their doses after correcting for the relative potency. For example, mixing 0.5× MIC of antibiotic A with 0.5× MIC of antibiotic B should produce a combined effect that is equivalent to 1× MIC of antibiotics A or B (when applied individually). Plots of the two-dimensional matrix of the cell viability data produce isoboles, *i.e.* lines of constant inhibition. The shape of the isoboles provides information about the interaction between the drugs. Linear (straight) isoboles indicate additive (non-interacting) compounds. Concave isoboles suggest a synergistic combination: lower concentrations of a combination of drugs inhibit as strongly as higher concentrations of the individual drugs. Antagonistic pairs produce convex isoboles. Finally, isoboles that are strongly skewed to one side reflect a suppressive interaction: one in which inhibition depends predominantly on the concentration of only one antibiotic in a mixture of two antibiotics. According to these definitions we determined the following types of interactions of pairs of antibiotics against *E. coli* ATCC 25922: antagonistic (ampicillin and chloramphenicol), suppressive (ampicillin and tetracycline), and additive (chloramphenicol and tetracycline). The result for the pair ampicillin–chloramphenicol corroborates well with the recent result of Cao *et al.*[11]

Identification of types of three pairwise interactions in a single experiment

To explore the application of the device for the rapid determination of interactions between antibiotics, we used it to screen all three pairwise interactions between antibiotics in a single experiment. We used three of the input reservoirs to deposit solutions of the three antibiotics at concentrations: ampicillin 3.15 mg L^{-1}, chloramphenicol 0.735 mg L^{-1} and tetracycline 0.231 mg L^{-1} (Fig. 7a). We created 63 droplets (volume of 2.1 μL) each of which contained 100 nL of a suspension of *E. coli* (7×10^6 CFU mL^{-1}) in culture media. The sequence of 63 drops consisted of three sub-sequences, each containing 21 droplets that were used to study the interaction of *E. coli* with one pair of antibiotics (Fig. 7b). Within each short (21 drops) sequence of microdroplets, the concentration of one antibiotic changed from 0 to $C_{1/2}$, where $C_{1/2}$ is the concentration of antibiotic at which the measured intensity of fluorescence from resorufin was equal to half the maximum value (Fig. 5c): $C_{1/2} = 3$, 0.7, 0.22 mg L^{-1} for ampicillin, chloramphenicol and tetracycline, respectively. In the sequence the concentration of one of the pairs of antibiotics was equal to $C^1 = (i-1)(C^1{}_{1/2}/20)$ where the index i ranged from 1 to 21. The concentration of the second antibiotic in the pair also changed linearly with i but in the opposite direction: $C^2 = (21-i)(C^1{}_{1/2}/20)$. The index of the droplets in the whole sequence is simply equal to $n = (j-1)21 + i$, where index j numbers the pairs of antibiotics: $j = 1$ corresponds to the pair of ampicillin and chloramphenicol, $j = 2$ to chloramphenicol and tetracycline and $j = 3$ to tetracycline and ampicillin.

We incubated the droplets for 3 h and measured the intensity of fluorescence emitted from resorufin. The shape of the curves demonstrated the relationships between the viability of bacteria and the chemical composition of microdroplets, and can be directly related to the shape of the isoboles on the maps of the interactions. Additive compounds should produce a straight line between end-points representing viability of bacteria in the presence of single antibiotics. Synergistic interactions are expected to produce curves of viability that are positioned below the straight line. Antagonistic interactions should result in higher viabilities of mixtures than a linear combination of the viabilities at the end points (Fig. 7c). Finally a suppressive interaction should result in a skewed viability curve. The results of our experiments reproduced these scenarios: ampicillin and tetracycline were antagonistic (Fig. 7d), chloramphenicol and tetracycline were additive (Fig. 7e) and ampicillin and chloramphenicol were suppressive (Fig. 7f).

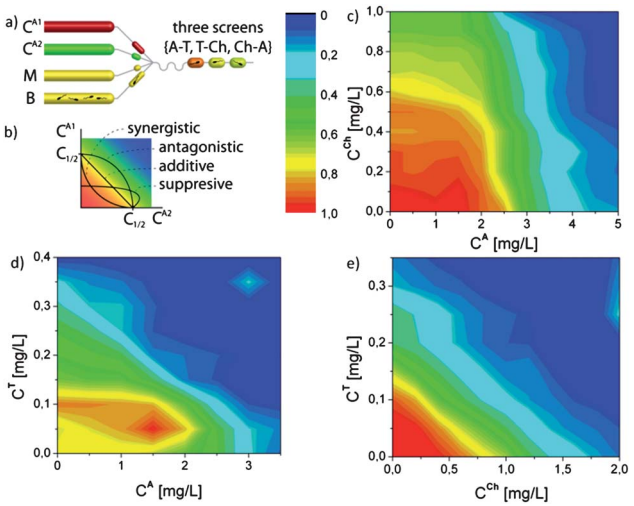

Fig. 6 A scheme depicting the composition of samples in the device reservoirs (a). The system enabled us to determine the interactions between pairs of antibiotics (b) and maps (11 × 11) of toxicity (C^A—ampicillin, C^{Ch}—chloramphenicol, C^T—tetracycline) (c–e). Each of these maps is an interpolation color fitting of data from 3 separate experiments. The standard deviation of this approximation is 3%.

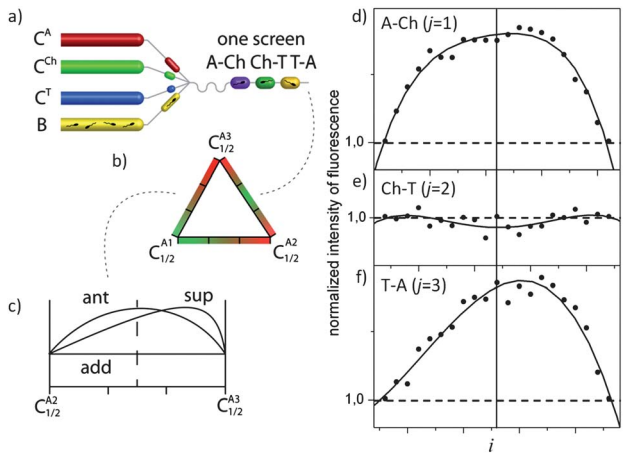

Fig. 7 A scheme depicting the composition of samples loaded onto the microfluidic chip (a). The system enabled us to measure interactions between pairs of antibiotics on the sides of the triangle spanned by the concentrations $C^A{}_{1/2}$, $C^{Ch}{}_{1/2}$, and $C^T{}_{1/2}$ (b and c) and to distinguish different types of interactions (d–f). Data points shown in insets (d–f) were normalized by a linear interpolation of the intensity of fluorescence between the values measured for individual antibiotics at their $C_{1/2}$ concentrations.

Conclusions

Classical microbiological methods

The most common techniques for testing antimicrobial susceptibility and determining MIC values hinge on measuring growth rates. Broth-dilution and disk-diffusion methods[37,38] are among the most commonly used techniques for determining the susceptibility of bacterial strains to antimicrobial agents. These methods are time-, labor- and reagent-consuming. For example, the techniques typically require overnight incubation of samples to achieve enough cells for bulk measurement. The workload of these assays can be minimized using several approaches, including automating liquid handling steps and incorporating multi-well plates. However, multi-well plates come with added challenges, including adhesion and evaporation, particularly when the volume of individual reactions is decreased to single microlitres.[39] PCR thermocyclers can be used to detect and identify the strain of pathogenic microorganisms within several hours,[40] however the relationship between the genotype of bacteria and their resistance to antibiotics is not always clear and restricts the use of PCR-based methods for the widespread determination of bacterial susceptibility to antibiotics.

Small samples

Microfluidics can address many of the current limitations of traditional microbiological assays and techniques by: (i) reducing the total volume of sample required to run an assay or screen; and (ii) providing an approach for multiplexing and performing assays quickly. However, flow through microchannels is commonly driven either by syringe pumps, where the sample is stored in a syringe and the dead volume of the syringe, needle, tubing and microchannel limits the minimal volume, or pressurized containers, where the dead volume of container and the volume of ducts limit the minimum volume. Dead volumes are typically in the range of millilitres to hundreds of microlitres in most experiments, and although only a small volume of sample is analyzed, the technique requires the user to have a much larger sample in hand.

Several solutions have been reported for the integration of various forms of sample aspiration with microfluidic protocols for manipulating droplets. For example, Clausell-Tormos *et al.*[41] presented a module that aspirates samples from the wells of multi-well plates *via* the use of a multichannel valve, splits samples, and merges them with a common reagent at a frequency of 0.33 Hz. Trivedi *et al.*[42] generated droplets (at 200 Hz) in a microfluidic flow-focusing junction from liquid flowing from a chromatography column and merged them with a reagent at a frequency of 20 Hz. Chen *et al.*[7] developed the *chemistrode* system that aspirates samples directly from a cell culture. The modification of this system by Liu *et al.*[9] enabled the aspiration of samples with small volume. Sun and Fang[43] presented an automated system for sampling from an Eppendorf tube. Du *et al.*[44] demonstrated a different system for aspirating samples from Eppendorf tubes, mixing them at known volume ratios, creating droplets from the mixtures, and depositing them into the wells of a multi-well plate.

The system that we report demonstrates an important improvement in the ease of handling small samples for performing high-throughput biological assays. The user deposits small volumes of samples (>1 microlitre) directly on chip using a pipette and runs an automated protocol on the samples.

Microfluidic methods for screening of reaction and incubation conditions

Microfluidic systems are becoming progressively more sophisticated for screening a range of reaction conditions in droplets. For example, Song and Ismagilov[45] reported a system for varying the composition of droplets by controlling the input flow rates in time. Damean *et al.*[46] used a gradient-generating device to create droplets of varied compositions and used this system to study an enzyme. Another way of testing multiple conditions in droplets is to create libraries of droplets with varied content and fluorescent coding.[47–49] Niu *et al.*[50] demonstrated the dilution of reagents in droplets across a concentration range that was four orders of magnitude. This automated design uses the geometry of the dilution chamber to define the ramp in the gradation of concentration. Sun and Fang[43] presented a technique for creation of static arrays of droplets containing a range of reagent concentrations.

Very recently Cao *et al.*[11] reported a system that automates the method proposed by Song and Ismagilov[45] of joining streams of different solutions immediately upstream of the droplet generator. By varying the rates of flow one can screen the composition space of the content of the droplets. Cao *et al.* used six computer-controlled pumps to generate segmented flow for high-throughput screening (about 3 Hz) of two, three, four and five dimensional matrixes of compositions of reagents, and applied the device to screen the toxicity of mixtures of ampicillin and chloramphenicol. This system presents an impressive combination of the number of dimensions in the composition space (up to five) that can be screened, the generation of droplets at a frequency of 3 Hz, and small mixture volumes (200–300 nL).

Our system complements this work by contributing several new dimensions: (i) it can analyze small volumes of liquids (solutions and suspensions), including samples that have a wide range of viscosities (and unknown viscosity); (ii) it manipulates volumes of liquid with high precision (standard deviation of the mean volume is <1%) and facilitates the preparation of combinations of reagents over a range of concentrations precisely; (iii) it enables users to easily exchange samples and to perform sequential screens rapidly; and (iv) it addresses each droplet in the sequence individually and facilitates screening the concentration space of different reagents and biologically active small molecules.

We believe that the short-term development of this automated microfluidic system—including the combining of features that have been introduced into other systems—will extend its capabilities for on-demand laboratory and diagnostic assays and play an important role in new areas of clinical microbiology. The system that we described here allows rapid formation of short sequences that probe two- or three-dimensional composition spaces. More complicated systems that alleviate the hydraulic feedback between the droplets already formed and the process of generation of new droplets (*i.e. via* the introduction of temporally modulated 'grounding' of the droplet generators to the atmospheric pressure) should also allow for continuous

generation of long (10^2 to 10^4) sequences of droplets that scan multi-dimensional spaces of chemical composition.

Methods

Fabrication of the chips

We fabricated microfluidic chips in a 5 mm thick sheet of polycarbonate (Macroclear, Bayer, Germany) using a CNC milling machine (MSG4025, Ergwind, Poland). The 5 mm thick polycarbonate form was bonded to a 2 mm thick plate by exposing both substrates to oxygen plasma and subsequently compressing them together (45 min, 130 °C, 0.4 MPa). We modified the surfaces of the microchannels by treating them with a solution of dodecylamine.[51] We created the world-to-device interface using steel capillaries (~4 cm, O.D. 0.8 mm, I.D. 0.65 mm, Mifam, Poland). We connected the device inlets to capillaries extending from the valves using short segments of Tygon® tubing (~1 cm, O.D. 0.91 mm, I.D. 0.25 mm, Ismatec, Switzerland).[31]

Automation

We delivered hexadecane from a pressurized reservoir through electromagnetic valves (V165, Sirai, Italy) *via* resistive steel capillaries (O.D. 400 μm, I.D. 205 μm, length 30 cm, Mifam, Poland). We controlled the pressure applied to the hexadecane reservoirs using a manual pressure regulator (Rexroth PR1-RGP) and monitored the pressure using a digital manometer (AZ 82100, AZ Instruments, Poland). The electromagnetic valves were controlled using a 24 V driver by connecting them to the analog outputs of a National Instrument card (NI PCI-6703) installed on a PC. We used custom written Lab View software to control the formation of droplets with a fixed volume (between 100 nL and 2 μL). Droplets were formed synchronously at T-junctions and transported to the merging chamber by the pressure driven flow of hexadecane. We coalesced microdroplets by applying an AC current across the chamber (200 Hz, ~1500 V, produced by the 10/10B-HS high-voltage power amplifier, TReK, USA).

Optical interrogation of droplets

We used a USB 2000+ Ocean Optics fiber optic spectrophotometer connected to the microfluidic channel *via* multimode fibers BFH22-365 (0.22 NA, spectral range: 190–1200 nm, 365 μm core). We inserted fibers into the chip and connected them to a light source and a detector. We used two illumination sources for measuring the absorption of light by microdroplets: (i) deuterium and halogen bulbs emitting a spectrum between $\lambda =$ 210 and 1700 nm (DH2000-FHS-DUV); and (ii) a green laser with $\lambda = 532$ nm (50 mW power) to excite resorufin. We used a Nikon SMZ1000 stereoscope coupled with a Photron Fast-Cam 1000k camera to image the formation and merging of droplets.

Microbiology

We used Mueller-Hinton (MH) broth (BD Biosciences, USA) for all of the experiments, as this culture medium is a standard for testing the antibiotic susceptibility of bacteria. All of our experience focused on the response of *E. coli* ATCC 25922 to antibiotics. We prepared a stock solution of cells in Luria-Bertani medium (BD Biosciences, USA) containing 30% (v/v) glycerol (Chempur, Poland) and froze them at −80 °C. Before the experiment, cells were streaked on Mueller-Hinton agar plates and incubated overnight. We picked individual colonies, used them to inoculate liquid broth, and cultured the cells at 37 °C overnight with shaking at 200 rpm. Aliquots of the overnight cultures were used to seed fresh liquid media and were grown to an absorbance of 0.1 ($\lambda = 600$ nm). In experiments for determining MICs we diluted the culture by 7.14× prior to transferring it to the inlet of the microfluidic chip. The suspension of bacteria was subsequently diluted 14× during the merging of droplets on-chip. Thus, the approximate starting concentration of bacteria inside the microdroplets incubating in the external tubing was $\sim 5 \times 10^5$ CFU mL^{-1}. In experiments in which we studied interactions between pairs of antibiotics, we started the incubation of mixtures at the same concentration of cells ($\sim 5 \times 10^5$ CFU mL^{-1}). In this experiment, bacteria were grown in the same way as for determination of MIC.

Antibiotics

We prepared antibiotic stocks of ampicillin and tetracycline hydrochloride using deionized water—for chloramphenicol we used a 50% (v/v) aqueous solution of ethanol—at a concentration that was 1000× more concentrated than in our experiments on-chip. All antibiotics were purchased from Roth (Germany). We sterilized antibiotic stock solutions by filtration. Due to instability of the ampicillin solution during freezing,[33] we prepared all stocks immediately prior to experiments. Before each experiment we diluted antibiotic stocks in MH broth to the desired concentration and transferred the samples to the inlets of the device. The concentration of antibiotics was subsequently reduced during the merging of droplets on-chip.

We used resazurin (Sigma-Aldrich, Poland) diluted in MH broth at a concentration of 44 μM as an indicator of cell viability and metabolism. To maintain a constant concentration of resazurin in the incubation mixtures, we added the compound to all solutions introduced into the device with the exception of the suspension of bacteria.

We used hexadecane (Alfa Aesar, Germany) containing 2% Span 80 (Sigma-Aldrich, Poland) as the continuous phase. To calibrate and verify the generation of binary mixtures of small molecules, we used aqueous solutions of dyes: tartrazine and methylene blue (both from Sigma-Aldrich, Poland), all at a concentration of 10 μM.

MIC measurements using the broth dilution technique

We used nine tubes containing 2 mL of MH broth medium admixed with bacteria (5×10^5 CFU mL^{-1}) and a tenth tube containing 4 mL of MH broth medium with the same concentration of bacteria and antibiotic at a concentration of 32 mg L^{-1}. We transferred 2 mL from the tenth tube to the ninth tube and we iterated this operation 10 times to create a two-fold gradient of antibiotic in the ten test tubes. We determined the MIC as the lowest concentration of antibiotics for which there was no visible growth of bacteria after 20 h of incubation.

Acknowledgements

This project operated within the Foundation for Polish Science Team Programme co-financed by the EU European Regional Development Fund and the Human Frontiers Science Program (RGY0069/2008). KCh acknowledges support from Iuventus Plus programme no. 2010 005270.

Notes and references

1 S. B. Levy and B. Marshall, *Nat. Med.*, 2004, **10**, S122–S129.
2 H. Goossens, M. Ferech, R. V. Stichele, M. Elseviers and E. P. Grp, *Lancet*, 2005, **365**, 579–587.
3 C. T. Keith, A. A. Borisy and B. R. Stockwell, *Nat. Rev. Drug Discovery*, 2005, **4**, 71–U10.
4 R. Chait, A. Craney and R. Kishony, *Nature*, 2007, **446**, 668–671.
5 M. Hegreness, N. Shoresh, D. Damian, D. Hartl and R. Kishony, *Proc. Natl. Acad. Sci. U. S. A.*, 2008, **105**, 13977–13981.
6 T. Bollenbach and R. Kishony, *Mol. Cell*, 2011, **42**, 413–425.
7 C. H. Chen, Y. Lu, M. L. Y. Sin, K. E. Mach, D. D. Zhang, V. Gau, J. C. Liao and P. K. Wong, *Anal. Chem.*, 2010, **82**, 1012–1019.
8 J. Q. Boedicker, L. Li, T. R. Kline and R. F. Ismagilov, *Lab Chip*, 2008, **8**, 1265–1272.
9 W. Liu, H. J. Kim, E. M. Lucchetta, W. Du and R. F. Ismagilov, *Lab Chip*, 2009, **9**, 2153–2162.
10 Y.-J. Eun, A. S. Utada, M. F. Copeland, S. Takeuchi and D. B. Weibel, *ACS Chem. Biol.*, 2011, **6**, 260–266.
11 J. Cao, D. Kürsten, S. Schneider, A. Knauer, M. Günther and M. Köhler, *Lab Chip*, 2012, **12**, 474–484.
12 Y. Schaerli and F. Hollfelder, *Mol. BioSyst.*, 2009, **5**, 1392–1404.
13 A. B. Theberge, F. Courtois, Y. Schaerli, M. Fischlechner, C. Abell, F. Hollfelder and W. T. S. Huck, *Angew. Chem., Int. Ed.*, 2010, **49**, 5846–5868.
14 K. Churski, P. Korczyk and P. Garstecki, *Lab Chip*, 2010, **10**, 816–818.
15 M. Chabert, K. D. Dorfman and J. L. Viovy, *Electrophoresis*, 2005, **26**, 3706–3715.
16 M. Zagnoni and J. M. Cooper, *Lab Chip*, 2009, **9**, 2652–2658.
17 K. Ahn, J. Agresti, H. Chong, M. Marquez and D. A. Weitz, *Appl. Phys. Lett.*, 2006, **88**, 264105.
18 T. Szymborski, P. M. Korczyk, R. Hołyst and P. Garstecki, *Appl. Phys. Lett.*, 2011, **99**, 094101.
19 S. L. Anna, N. Bontoux and H. A. Stone, *Appl. Phys. Lett.*, 2003, **82**, 364–366.
20 P. Garstecki, I. Gitlin, W. DiLuzio, G. M. Whitesides, E. Kumacheva and H. A. Stone, *Appl. Phys. Lett.*, 2004, **85**, 2649–2651.
21 P. Garstecki, H. A. Stone and G. M. Whitesides, *Phys. Rev. Lett.*, 2005, **94**, 164501.
22 W. Lee, L. M. Walker and S. L. Anna, *Phys. Fluids*, 2009, **21**, 032103.
23 T. Thorsen, R. W. Roberts, F. H. Arnold and S. R. Quake, *Phys. Rev. Lett.*, 2001, **86**, 4163–4166.
24 P. Garstecki, M. J. Fuerstman, H. A. Stone and G. M. Whitesides, *Lab Chip*, 2006, **6**, 437–446.
25 G. F. Christopher, N. N. Noharuddin, J. A. Taylor and S. L. Anna, *Phys. Rev. E: Stat., Nonlinear, Soft Matter Phys.*, 2008, **78**, 036317.
26 M. De Menech, P. Garstecki, F. Jousse and H. A. Stone, *J. Fluid Mech.*, 2008, **595**, 141–161.
27 V. van Steijn, C. R. Kleijn and M. T. Kreutzer, *Phys. Rev. Lett.*, 2009, **103**, 214501.
28 V. van Steijn, C. R. Kleijn and M. T. Kreutzer, *Lab Chip*, 2010, **10**, 2513–2518.
29 Z. Nie, M. Seo, S. Xu, P. C. Lewis, M. Mok, E. Kumacheva, G. M. Whitesides, P. Garstecki and H. A. Stone, *Microfluid. Nanofluid.*, 2008, **5**, 585–594.
30 J. Guzowski, P. M. Korczyk, S. Jakiela and P. Garstecki, *Lab Chip*, 2011, **11**, 3593–3595.
31 P. M. Korczyk, O. Cybulski, S. Makulska and P. Garstecki, *Lab Chip*, 2011, **11**, 173–175.
32 S. Jakiela, S. Makulska, P. M. Korczyk and P. Garstecki, *Lab Chip*, 2011, **11**, 3603–3608.
33 J. M. Andrews, *J. Antimicrob. Chemother.*, 2001, **48**, 5–16.
34 M. Wikler, F. Cockerill, W. Craig, M. Dudley, G. Eliopoulos, D. Hecht, J. Hindler, D. Low, D. Sheehan, F. Tenover, J. Turnidge, M. Weinstein, B. Zimmer, M. Ferraro and J. Sewnson, *Performance Standards for Antimicrobial Susceptibility Testing; Seventeenth Informational Supplement*, Clinical and Laboratory Standards Institute, Wayne, Pennsylvania, 2007.
35 P. J. Yeh, M. J. Hegreness, A. P. Aiden and R. Kishony, *Nat. Rev. Microbiol.*, 2009, **7**, 460–466.
36 S. Loewe, *Ergebnisse der Physiologie*, 1928, **27**, 47–187.
37 A. W. Bauer, W. M. M. Kirby, J. C. Sherris and M. Turck, *Am. J. Clin. Pathol.*, 1966, **45**, 493.
38 D. R. Stalons and C. Thornsberry, *Antimicrob. Agents Chemother.*, 1975, **7**, 15–21.
39 A. Dove, *Nat. Biotechnol.*, 1999, **17**, 859–863.
40 M. J. Espy, J. R. Uhl, L. M. Sloan, S. P. Buckwalter, M. F. Jones, E. A. Vetter, J. D. C. Yao, N. L. Wengenack, J. E. Rosenblatt, F. R. Cockerill and T. F. Smith, *Clin. Microbiol. Rev.*, 2006, **19**, 165.
41 J. Clausell-Tormos, A. D. Griffiths and C. A. Merten, *Lab Chip*, 2010, **10**, 1302–1307.
42 V. Trivedi, A. Doshi, G. K. Kurup, E. Ereifej, P. J. Vandevord and A. S. Basu, *Lab Chip*, 2010, **10**, 2433–2442.
43 M. Sun and Q. Fang, *Lab Chip*, 2010, **10**, 2864–2868.
44 W.-B. Du, M. Sun, S.-Q. Gu, Y. Zhu and Q. Fang, *Anal. Chem.*, 2010, **82**, 9941–9947.
45 H. Song and R. F. Ismagilov, *J. Am. Chem. Soc.*, 2003, **125**, 14613–14619.
46 N. Damean, L. F. Olguin, F. Hollfelder, C. Abell and W. T. S. Huck, *Lab Chip*, 2009, **9**, 1707–1713.
47 H. N. Joensson, M. L. Samuels, E. R. Brouzes, M. Medkova, M. Uhlen, D. R. Link and H. Andersson-Svahn, *Angew. Chem., Int. Ed.*, 2009, **48**, 2518–2521.
48 E. Brouzes, M. Medkova, N. Savenelli, D. Marran, M. Twardowski, J. B. Hutchison, J. M. Rothberg, D. R. Link, N. Perrimon and M. L. Samuels, *Proc. Natl. Acad. Sci. U. S. A.*, 2009, **106**, 14195–14200.
49 J.-C. Baret, Y. Beck, I. Billas-Massobrio, D. Moras and A. D. Griffiths, *Chem. Biol.*, 2010, **17**, 528–536.
50 X. Niu, F. Gielen, J. B. Edel and A. J. deMello, *Nat. Chem.*, 2011, **3**, 437–442.
51 P. Jankowski, D. Ogonczyk, A. Kosinski, W. Lisowski and P. Garstecki, *Lab Chip*, 2011, **11**, 748–752.